ISSN : 1978-774X

STUDY OF SHAFT POSITION IN GAS TURBINE JOURNAL BEARING

Rizky Arman, Iman Satria

Mechanical engineering Dept. Faculty of Industrial Technolgy,
Bung Hatta University, Padang 25143, Indonesia
rizky.arm@gmail.com

ABSTRACT

Bearings provide the primary interface between the moving and the stationary parts of a machine. Although the seal and the process fluids (or magnetic fields) coexist, the bearings provide the majority of the stiffness and damping for the moving assembly. It is understandable that dynamic forces developed on the moving part are transmitted to the stationary part across these main support bearings. The forces may be the static radial loads due to the rotor weight, or they may be dynamic forces due to mechanisms such as mass unbalance. In either case, the radial bearings must carry the applied loads, or the machine will fail. In most cases, it is technically difficult (if not impossible) to directly check the validity or accuracy of the computed bearing coefficients. However, each calculation must conclude with a force balance, plus a position balance of the journal within the bearing clearance. It is reasonable to believe that if the calculated eccentricity position is correct, than the other computed parameters are also representative of the bearing characteristics [a]. Since journal within an oil film bearing can be measured directly with proximity probes, it is logical perform a check of the analytical prediction versus actual machine data. For this case history, consider a group of four single shaft gas turbines that operate between 5,000 and 5,350 RPM. These units are rated at 40,000 HP, and they are used to drive high pressure centrifugal compressors through a single helical gear box. The shaft sensing proximity probes are mounted at ±450 from the true vertical centerline. At turbine inlet end#1 bearing, the probes are mounted above the shaft. Conversely, at the exhaust end #2 bearing, the probes are located below the shaft.
Key words: journal bearing, gas turbine, proximity probes.

1. INTRODUCTION

Bearings are used to prevent friction between parts during relative movement. In machinery they fall into two primary categories: anti-friction or rolling element bearings and hydrodynamic journal bearings. The primary function of a bearing is to carry load between a rotor and the case with as little wear as possible. This bearing function exists in almost every occurrence of daily life from the watch on your wrist to the automobile you drive to the disk drive in your computer. In industry, the use of journal bearings is specialized for rotating machinery both low and high speed [a], [b].

Fluid film bearings are the most widely used plain bearing. They rely on lubricant viscosity to separate the bearing surfaces. The rotating shaft drags the lubricant around forming a supporting wedge. These bearings usually need a lubrication system. The continuous lubrication acts to cool the bearing allowing high shaft speeds and heavy loads. Industrial machinery with high horsepower and high loads, such as steam turbines, centrifugal compressors, pumps and motors, utilize journal bearings as rotor supports. One of the basic purposes of a bearing is to provide a frictionless environment to support and guide a rotating shaft. Properly installed and maintained, journal bearings have essentially infinite life.

In most cases, it is technically difficult (if not impossible) to directly check the validity or accuracy of the computed bearing coefficients. However, each calculation must conclude with a force balance, plus a position balance of the journal within the bearing clearance. It is reasonable to believe that if the calculated eccentricity position is correct, than the other computed parameters are also representative of the bearing characteristics. Since journal within an oil film bearing can be measured directly with proximity probes, it is logical perform a check of the analytical prediction versus actual machine data.

2. THEORETICAL BACKGROUND

A journal bearing, simply stated, is a cylinder which surrounds the shaft and is filled with some form of fluid lubricant. In this bearing a fluid is the medium that supports the shaft preventing metal to metal contact. The most common fluid used is oil, with special applications using water or a gas. This application note will concentrate on oil lubricated journal bearings [b],[c],[d]. Hydrodynamic principles, which are active as the shaft rotates, create an oil wedge that supports the shaft and relocates it within the bearing clearances. In a horizontally split bearing the oil wedge will lift and support the shaft, relocating the centerline slightly up and to one side into a normal attitude position in a lower quadrant of the bearing. The normal attitude angle will depend upon the shaft rotation direction with a clockwise rotation having an attitude angle in the lower left quadrant. External influences, such as hydraulic volute pressures in pumps or generator electrical load can produce additional relocating forces on the shaft attitude angle and centerline position. An additional characteristic of journal bearings is damping. This type of bearing provides much more damping than a rolling element bearing because of the lubricant present. More viscous and thicker lubricant films provide higher damping properties. As the available damping increases, the bearing stability also increases. A stable bearing design holds the rotor at a fixed attitude angle during transient periods such as machine startups/shutdowns or load changes. The damping property of the lubricant also provides an excellent medium for limiting vibration transmission. Thus, a vibration measurement taken at the bearing outer shell will not represent the actual vibration experienced by the rotor within its bearing clearances.

The bearing inner surface is covered with a softer material, commonly called *babbit*. *Babbit*, which is a tin or lead based alloy, has a thickness that can vary from 1 to 100 mils depending upon the bearing diameter. A *babbit* lining provides a surface which will not mar or gouge the shaft if contact is made and to allow particles in the lubricant to be imbedded in the liner without damaging the shaft. Journal bearings have many differing designs to compensate for differing load requirements, machine speeds, cost, or dynamic properties. One unique disadvantage which consumes much research and experimentation is an instability which manifests itself as oil whirl and oil whip. Left uncorrected, this phenomenon is catastrophic and can destroy the bearing and rotor very quickly. Oil whip is so disastrous because the rotor cannot form a stable oil wedge consequently allowing metal to metal contact between the rotor and the bearing surface. Once surface contact exists the rotor begins to precess, in a reverse direction from rotor rotation direction, using the entire bearing clearance. This condition leads to high friction levels which will overheat the bearing *babbit* metal that leads to rapid destruction of the bearing, rotor journal, and the machine seals. Some common designs employed are lemon bore, pressure dam, and tilt pad bearings. These designs were developed to interrupt and redirect the oil flow path within the bearing to provide higher bearing stabilities. Journal bearings installed in industrial machinery today generally fall into two categories: full bearings and partial arc bearings. Full bearings completely surround the shaft journal with many differing geometries such as elliptical, lobed, or pressure dam configurations and usually are two pieces, mated at a split line. Partial arc bearings have several individual load bearing surfaces or pads and are made up of numerous adjustable components [e], [f].

Use of journal bearings is also an advantage in many applications when it comes to maintenance. Most fluid film bearings are split and rotor removal is not required to inspect and replace. While split rolling element bearings are also available they are costly and not common. Journal bearing fatigue damage is usually visible at an early stage and allows for better diagnostics of failure modes so that corrective action can be taken to prevent recurrence. The operating range for different types of bearing is shown in Figure 1.

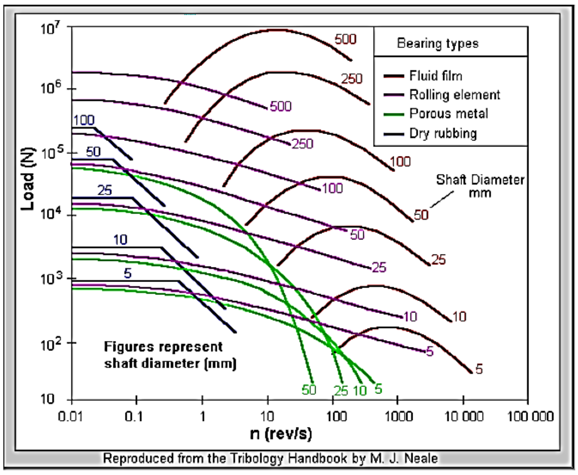

Figure 1 Operating ranges for different types of bearing

3. RESEARCH METHOD: STATIC AND DYNAMIC LOAD CARRYING CAPACITY

In the development of analytical machinery models, there is always a temptation to begin the project with a detailed rotor analysis. However, the machinery diagnostician soon discovers that bearing characteristics must be defined and included within the rotor model. In some cases, such as the optimization of a mechanical system, many different bearing types may be considered with different rotor models. Hence, it is often an iterative procedure to determine the proper combination of bearings and rotor configuration. One of the easiest and informative starting points is the determination of the static shaft loading upon the planar area of the bearing [g], [h].

The Basic Static Load Rating given for each bearing in bearing catalogues is based on the stationary axial and radial forces acting on the bearing. When bearings are subject to both radial and axial loadings the equivalent static load must be found thus:

$$Po = XoFr + YoFa \qquad (1)$$

If only radial forces act then;

$$Po = Fr \qquad (2)$$

Where
Po = The equivalent static bearing load (*N*)
Fr = static radial load on the bearing (*N*)
Fa = static axial load on the bearing (*N*)
Xo = static radial factor
Yo = static axial factor
(The values of Xo & Yo are given in the Bearing Data). The Basic Static Load Rating Co can be calculated from:

$$Co = SoPo \qquad (3)$$

where
Co = basic load rating (*N*)
So = static safety factor
Po = equivalent static bearing load (*N*)

Values of *So* depend on the type of bearing and the requirements regarding quiet running. If the bearing is stationary for long periods or rotates slowly and is subject to shock loads then the bearing selection procedure is based on this basic load rating. Values of *Co* for each bearing are quoted in the bearing catalogues. Choose a bearing whose quoted value for *Co* is equal to the required value of *Co* calculated above, and static safety factor is shown at Table 1.

Table 1. Guidelines for static safety factor

	noise unimportant		normal running		quite running	
	ball	roller	ball	roller	ball	roller
smooth loading	0.5	1	1	1.5	2	3
normal loading	0.5	1	1	1.5	2	3.5
shock loading	>= 0.5	>= 0.5	>= 0.5	>= 3	>= 2	>= 4

The dynamic load carrying capacity of a bearing is dependent on the dynamic forces acting on the bearing as well as the basic static forces. The first step is therefore to calculate the Static Load Rating before continuing with the following procedure. If the bearing is subject to radial and axial forces then an equivalent dynamic bearing load must be calculated:

$$P = XFr + YFa \qquad (4)$$

P = The equivalent dynamic bearing load (*N*)
Fr = static radial load on the bearing (*N*)
Fa = static axial load on the bearing (*N*)
X = radial factor
Y = axial factor

When *Fa* = 0 or *Fa* is relatively small up to a limiting case of *Fa/Fr = e* (where e is a certain limiting value) then:

$$P = Fr \qquad (5)$$

(The values of *X, Y* & *e* are given in the Bearing Data)

Once a value for the equivalent dynamic bearing load is obtained it can be used to calculate the dynamic load rating of the bearing. This value is used to select the bearing. Each bearing in the bearing catalogue has a quoted value for dynamic load rating and so a bearing should be chosen that has a higher rating than the one calculated. The dynamic load rating that is quoted in the catalogues for each bearing is dependent on the required life of the bearing and the equivalent dynamic bearing load (P). The ISO equation for basic rating life is:

$$L_{10} = \left(\frac{C}{P}\right)^{p} \; or \; C = PL_{10}{}^{1/p} \qquad (6)$$

Where

L = basic rated life, Millions of revolutions
C = basic dynamic load rating
P = equivalent dynamic bearing load
p = exponent in the life equation (3 for all ball bearings and 10/3 for all other roller bearings)

The basic rated life (defined as the number of revolutions that 90% of a group of identical bearings would be expected to achieve) is determined from the length of life that is required of the bearing. Typical life expectancies of required of various machines are given below.

Table 2. Life expectancies of required of various machines

Machine Usage	Hours
intermittent- domestic machines	300-3000
short periods- hand tools,	
construction machines	3000-8000
high reliability for short periods-	
lifts, cranes	8000-12000
8 h/day partial use gears, motors	10000-25000
8 h/day full use machine tools,	20000-30000
fans	40000-50000
continuous use	

4. RESULT AND DISCUSSION: CASE HISTORY OF SHAFT POSITION IN GAS TURBINE JOURNAL BEARING

In most cases, it is technically difficult (if not impossible) to directly check the validity or accuracy of the computed bearing coefficients. However, each calculation must conclude with a force balance, plus a position balance of the journal within the bearing clearance. It is reasonable to believe that if the calculated eccentricity position is correct, than the other computed parameters are also representative of the bearing characteristics. Since journal within an oil film bearing can be measured directly with proximity probes, it is logical perform a check of the analytical prediction versus actual machine data [a] [i],[j],[k].

For this case history, consider a group of four single shaft gas turbines that operate between 5,000 and 5,350 RPM. These units are rated at 40,000 HP, and they are used to drive high pressure centrifugal compressors through a single helical gear box. The shaft sensing proximity probes are mounted at ±450 from the true vertical centerline as shown in Figure 2. At turbine inlet end#1 bearing, the probes are mounted above the shaft. Conversely, at the exhaust end #2 bearing, the probes are located below the shaft [a].

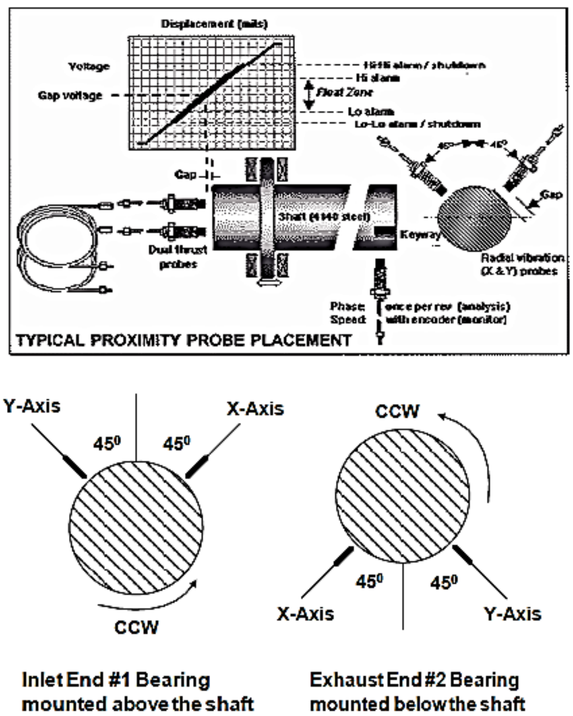

Figure 2 Measurement with proximity probes on shaft

The eight inch diameter journals are supported in elliptical bearings. These bearings have an average vertical diametrical clearance of 16 Mils (0.016

inches), and a normal horizontal diameter clearance of 32 Mils. These physical dimensions are consistent with 2:1 clearance.

The shaft centerline position for these machine journals was determined by measuring the proximity probe DC gap voltages at a stop condition, and at full speed. The difference between these DC voltages is divided by the transducer scale factor to determine the position change in the direction of each transducer. This X-Y change in radial position may be plotted on a graph that display the bearing clearance, plus the calculated journal position in the X and Y direction [l].

Fig.3 depicts the radial journal positions for the turbine inlet bearings. Shaft centerline location for the A unit were obtained on different dates, and at slightly different speeds varying between 5,100 and 5,340 RPM. Three additional machines identified as the B, C, and D units are also included in these survey. Speeds for these last three units varied between 5,010 and 5,350 RPM. It is noted that excellent agreement has been achieved between the calculated position at 5,340 RPM, and the six sets of field data.

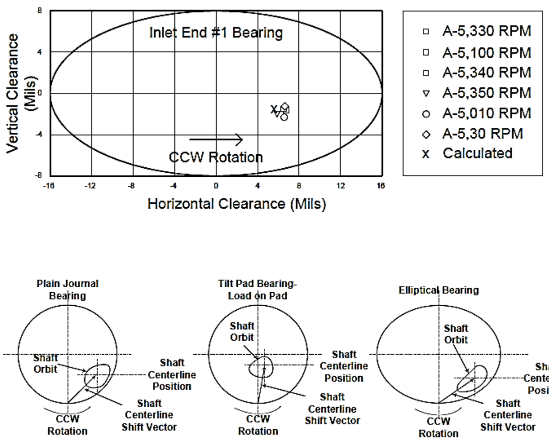

Figure 3 Shaft centerline position on journal bearings at inlet end #1

The same position information for the exhaust end #2 bearing as contained in Figure 4. Notice that the scatter of data is much greater at this bearing, and the deviations from the calculated position are substantial. Initially, it might be concluded that the theory does not support the actual machinery behaviour. However, a partial explanation for these aberrations resides within the characteristics of the proximity probes, and the companion drivers are sensitive to operating temperature. The temperature limit specification for this specific probe and cable was 3500F; and the oscillator-demodulator operating limit was specified as 1500F for a standard unit, or 2120F for extended temperature range version.

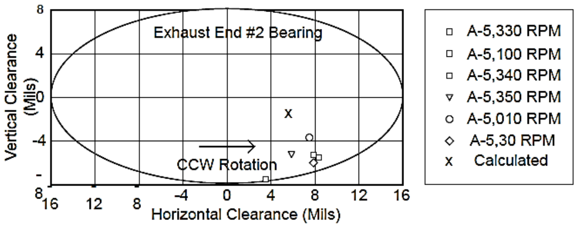

Figure 4 Shaft centerline position on journal bearings at exhaust end #2

As shown in Figure 2, the exhaust end probes are mounted outboard of the #2 bearing, and below the horizontal centerline. These probes are subjected to a high temperature environment that can easily heat the transducer to temperatures in excess of 2000F. the oscillator-demodulators are mounted in an explosion proof housing. Although a heat shield is installed between the turbine exhaust and this box, the electrical components often operate at temperatures above 1300F. Thus, the exhaust end probes, cables, and drivers are all exposed to elevated temperatures that affect the calibration curve slope.

For many years, the instrumentation vendors have recognized that operating temperature will influence probe calibration. For instance, Fig.5 depicts the variation in calibration curves at temperatures of 75, 200, and 3500F. This data was published by the manufacturer of the proximity probes installed on these particular gas turbines. The plotted data is for a 0.300 inch diameter probe. Larger excursions are normally exhibited by smaller diameter probe tips. From this family of curves, it is clear that the calibration curve will bend downward as the temperature increase. At 2000F, the calibration curve is nominally 0.5 volts below the normal curve for gaps in the vicinity of -9.0 to -10.0 volts DC. Hence, for a given distance between the probe and shaft, the output DC voltage from the Proximitor® is reduce by about 0.5 volts. Since the measurement system operates with negative bias, the gap voltages are likewise negative.

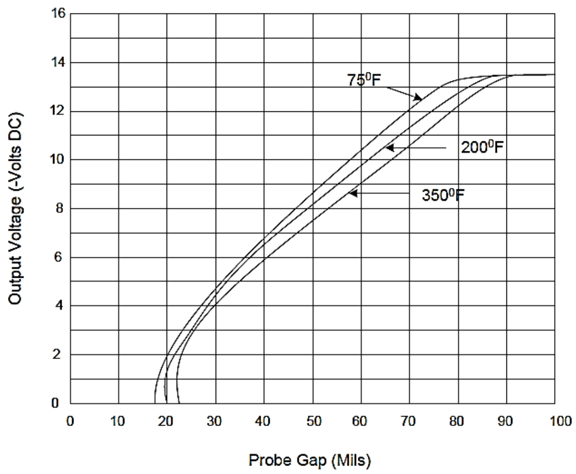

Figure 5 Variation in calibration curves at temperatures of 75, 200, and 3500F

The correction for this temperature behaviour requires adding the incremental voltage to the Proximitor® output voltage. Thus, the measured output DC voltage should be corrected by -0.5 volts DC to yield a temperature compensated value. Specifically, Table 3 summarizes the cold (at stop) gap voltages, plus the hot (running) gap voltage or the B machine.

Table 3. Direct Proximity Probe Gap Voltages At Turbine Exhaust End #2 Bearing

Probe and Angular Location	Cold Gap Voltage	Hot Gap Voltage	Differential Gap Voltage	Differential Position
Y-Axis @315⁰	-9.66 volts DC	-9.23 volts DC	+0.43 volts DC	+2.15 Mils
X-Axis @225⁰	-9.23 volts DC	-10.47 volts DC	-1.24 volts DC	-6.20 Mils

The differential gap voltages are merely the cold minus the hot gap voltages at the turbine exhaust bearing. Dividing the Y-axis (vertical) probe differential gap voltage by the normal transducer sensitivity of 0.2 Volts/Mil) yields a displacement change of 2.15 Mils towards the probe. Similarly, the X-axis (horizontal) transducer exhibits a -1.24 volt change, which is equivalent to a 6.20 Mil position shift away from the probe. This is equivalent to an overall shaft vector shift of 6.56 Mils at 260 from the cold to the hot position.

However, if the measured hot probe gap voltages are corrected by -0.5 volts DC to compensate for the transducer temperature sensitivity, the result are shown in Table 4. The initial cold gap voltages (zero speed) remain the same as before.

The displacement shift is again determined by dividing the differential gap voltages by 0.2 Volts/Mil to determine the distance shift. For the Y-axis probe, this yields a displacement change of 0.35 Mils away from the probe. The X-axis transducer now displays a -1.74 volt change, which is equal to an 8.70 Mil position shift away from the transducer. The total shift of the journal centerline position is therefore equivalent to a vector shift of 8.71 Mil at 470 (cold to hot position). Thus, the temperature correction reveals that the shaft is really riding higher in the bearing than the uncorrected data revealed.

Table 4. Corrected Proximity Probe Gap Voltages At Turbine Exhaust End #2 Bearing

Probe and Angular Location	Cold Gap Voltage	Hot Gap Voltage	Differential Gap Voltage	Differential Position
Y-Axis @315⁰	-9.66 volts DC	-9.73 volts DC	-0.07 volts DC	-0.35 Mils
X-Axis @225⁰	-9.23 volts DC	-10.97 volts DC	-1.74 volts DC	-8.70 Mils

Correcting each of the hot gap voltages from the initial shaft centerline diagram produces the journal positions presented in Fig.6. Again, the exhaust end probes are mounted on the bottom of the shaft, and the corrected DC voltages reveal a shaft rise.

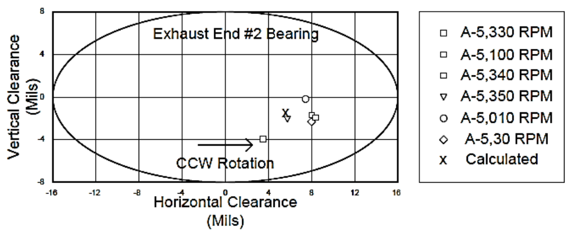

Figure 6 Corrected Proximity Probe Gap Voltages At Turbine Exhaust End #2 Bearing

It is evident that agreement between the calculated and measured journal position has been significantly improved by this simple probe gap temperature correction. The remaining deviations in measured radial position between both ends of the turbine may now be attributed to the presence of external loads, moments, or other influences acting upon the shaft.

Since the inlet end #1 Bearing is adjacent to the accessory coupling, vary little torque is transmitted during normal operation. Thus, the presence of external forces, and misalignment loads are minimal at the front end bearing. As previously observed, the measured positions agree very well with the theoretical calculations that consider only the load due to the applied journal weight.

5. CONCLUSION

However, at the gas turbine exhaust end bearing, the full power output from the turbine is transmitted across the load coupling. Dependent upon coupling type, alignment position and associated external forces, the actual journal location would probably deviated from the predicted eccentricity that was computed with only the journal weight. In fact, the reverse statement might also be appropriate. That is, since the exhaust end shaft centerline position agrees with the computed location, the influence of external forces may be considered to be minimal (i.e., indicative of a well-aligned Load coupling).

Overall, the eccentricity calculations at both ends of the turbine appear to be realistic and representative of average machine behavior. This correlation between the measured journal positions, and the computed equilibrium location is considered to be supportive of the accuracy of the analytical fluid film bearing calculations. Similar measurements and comparisons with calculated results may be performed at other speeds or different oil supply conditions. In most cases there should be a respectable correlation between the measured and the calculated shaft centerline position. This technique may also be used as a diagnostic tool. For example, if the measured shaft operating position is substantially different from the calculated position, the diagnostician should give strong consideration to the presence of internal or external shaft preloads.

6. REFERENCES

(a) P. Pennacchi and A. Vania, (2011). "Analysis of the instability phenomena caused by steam in high-pressure turbines," vol. 18, pp. 593–612.
(b) M. E. Leader, "Understanding Journal Bearings."
(c) D. J. Salamone, (1984). "Journal Bearing Design Types And Their Applications To Turbomachinery by," pp. 179– 190.
(d) "Bearing Supports from Automotion Components."
(e) M. He, C. H. Cloud, and J. M. Byrne, (2005). "Fundamentals Of Fluid Film Journal Bearing Operation And Modeling."
(f) W. B. Rowe, K. Cheng, and D. Ives, (1991). "A knowledge-based system for the selection of fluid film journal bearings," *Tribol. Int.*, vol. 24, no. 5, pp. 291–297.
(g) J. D. Irwin, (2001). *Mechanical Engineer ' s Handbook Academic Press Series in Engineering Series Editor*.
(h) J. D. Irwin, (2001). *Mechanical Engineer ' s Handbook*.
(i) C. Jackson, "by," pp. 73–86, 1960.
(j) G. F. Simmons, (2013). *Journal Bearing Design , Lubrication and*.
(k) K. R. Guy and D. A. Services, (2007). "11 Problems – 11 Solutions," no. March, pp. 16–22.
(l) J.D. McHugh, "principles of turbomachinery bearings.pdf."

AUTHOR BIOGRAPHIES

Rizky Arman is a lecturer in Mechanical Engineering Dept., Faculty of Industrial Technology, Bung Hatta University, Jakarta. She received his Master degree of Mechanical Engineering from Institut Technology Bandung in 2005. His research interests are in the area of Machine Construction, Vibration, Kinematics and Dynamics, Design and Simulation. He is a member of The Institution of Engineers Indonesia (PII). His email address is <rizky.arm@gmail.com>